# Possible influences of Asian dust aerosols on cloud properties and radiative forcing observed from MODIS and CERES

Jianping Huang,[1] Patrick Minnis,[2] Bing Lin,[2] Tianhe Wang,[1] Yuhong Yi,[3] Yongxiang Hu,[2] Sunny Sun-Mack,[4] and Kirk Ayers[3]

[1]   The effects of dust storms on cloud properties and Radiative Forcing (RF) are analyzed over Northwestern China from April 2001 to June 2004 using data collected by the MODerate Resolution Imaging Spectroradiometer (MODIS) and Clouds and the Earth's Radiant Energy System (CERES) instruments on the Aqua and Terra satellites. On average, ice cloud effective particle diameter, optical depth and ice water path of cirrus clouds under dust polluted conditions are 11%, 32.8%, and 42% less, respectively, than those derived from ice clouds in dust-free atmospheric environments. Due to changes in cloud microphysics, the instantaneous net RF is increased from $-161.6$ W/m$^2$ for dust-free clouds to $-118.6$ W/m$^2$ for dust-contaminated clouds. **Citation:** Huang, J., P. Minnis, B. Lin, T. Wang, Y. Yi, Y. Hu, S. Sun-Mack, and K. Ayers (2006), Possible influences of Asian dust aerosols on cloud properties and radiative forcing observed from MODIS and CERES, *Geophys. Res. Lett.*, *33*, L06824, doi:10.1029/2005GL024724.

## 1.   Introduction

[2]   Dust storms that blanket East Asia have serious impacts on the global climate system. These storms originate in the Taklamakan Desert of China and the Gobi Desert of China and Mongolia and occur most frequently in late winter and early spring. The dust aerosols not only reflect the incoming solar radiation to space, but also modify cloud properties by changing the number concentration of cloud droplets, which alters both cloud optical depth and cloud lifetime [*Twomey et al.*, 1984; *Ackerman et al.*, 2000]. In addition, the aerosols can affect the radiative heating structure of the atmosphere, thereby changing the clouds and atmospheric general circulation.

[3]   Recently, special attention has been dedicated to cloud interactions with desert aerosol particles [*Bréon et al.*, 2002; *DeMott et al.*, 2003]. *Rosenfeld et al.* [2001] found that clouds forming within desert dust contain small droplets and produce little precipitation by drop coalescence. *Levi and Rosenfeld* [1996] observed similar increase in ice nuclei concentrations during dust storm periods in Israel. The action of Saharan dust particles as ice nuclei was even used to explain the impacts of cloud seeding experiments in Israel [*Rosenfeld and Nirel*, 1996].

[4]   Despite the fact that the Taklamakan and Gobi Deserts are major sources of dust aerosols, there have been few studies focusing on the effect of Asian dust aerosols on clouds, especially ice cloud properties and RF. This study investigates the influence of Asian dust on ice cloud properties using the MODIS and CERES scanner data. The effect of dust aerosols on clouds is evaluated by comparing the properties and RF of dust-free and dusty clouds. This assessment should lead to a better understanding of the interactions among dust aerosols, clouds, and radiation fields.

## 2.   Data and Methodology

[5]   The Visible-Infrared-Solar-infrared-Split-window Technique (VISST) was used to derive daytime cloud properties from Aqua and Terra MODIS data taken between April 2001 and June 2004. VISST is a 4-channel update of the retrieval algorithm of *Minnis et al.* [1995, 1998]. The retrieved cloud properties include cloud effective droplet radius ($r_e$) or ice crystal diameter (De), optical depth ($\tau$), effective cloud temperature (Te), and water path (WP). Cloud WP retrievals are calculated from the cloud optical depth and effective particle size estimated from the VISST. Flux measurements from CERES are used to estimate the instantaneous RF. The CERES instruments measure broadband radiances at the Top-Of-Atmosphere (TOA) in three spectral regions ($0.2-5.0$ $\mu$m; $8-14$ $\mu$m; $5-100$ $\mu$m) at a spatial resolution of about 20 km at nadir. The CERES Meteorological, Ozone, and Aerosol (MOA) data are used to analyze meteorological conditions.

## 3.   Analysis and Results

[6]   Figure 1a shows images from MODIS data for a dust storm case on 27 March 2004 over Northwestern China. The existence of dust enhances the reflectance as seen in the true-color composite image (Figure 1a). *Ackerman* [1997] showed that the brightness temperature (BT) difference between the 11 and 12 $\mu$m channels (T45) is negative for dust because dust layers have a higher emissivity at 12 $\mu$m than at 11 $\mu$m. The BT difference is affected not only by the dust optical thickness, but by the type of dust [*Sokolik et al.*, 1998] and the particular characteristics of the 11 and 12-$\mu$m channels [*Sokolik*, 2002]. In a detailed case study, *Gu et al.* [2003] demonstrated that the MODIS T45 can be used to detect Asian dust and to retrieve the aerosol particle size and mass loading. This sensitivity is clearly seen in Figure 1b where the clouds are easily distinguishable from the dust in the T45 image. The average T45 value is less than $-2.0$ K for a pure dust region and larger than 0 K in the cloudy

---

[1]College of Atmospheric Sciences, Lanzhou University, Lanzhou, China.
[2]NASA Langley Research Center, Hampton, Virginia, USA.
[3]Analytical Services & Materials, Inc., Hampton, Virginia, USA.
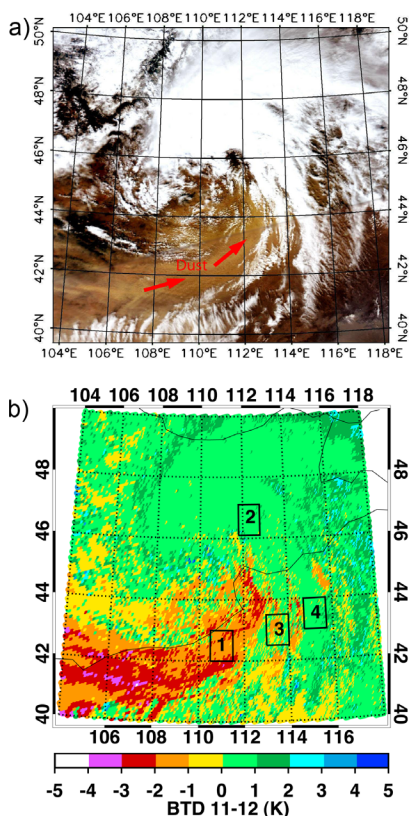[4]Science Applications International Corporation, Hampton, Virginia, USA.

**Figure 1.** (a) The true color composite over Northwest China, in which three channels, 0.65, 0.56 and 0.47μm, are associated with red, green and blue colors, respectively. (b) The BT difference between 11 and 12 μm channels (T45). Box 1 is the DUST region, box 2 the CLD region, box 3 the PCOD region, and box 4 the COD region, respectively.

regions. In dusty areas with clouds, the T45 signals from dust and clouds tend to cancel each other and are not very useful for cloud identification.

[7] To detect cloud modifications induced by dust aerosols, four regions are selected to represent the dusts and clouds in different environments. Box 1 (hereafter DUST) in Figure 1b represents the cloud-free dust region. Box 2 (hereafter, CLD) denotes an area where clouds occurred in a dust-free atmosphere. Box 3 (hereafter, PCOD) includes partial clouds in a dusty region. The clouds in the PCOD region are actually solid-deck clouds although they do not fully cover the whole PCOD region. Box 4 (hereafter, COD) represents overcast clouds in dusty conditions. The CLD and COD regions are selected based on observations from 701 surface meteorological stations in China and Mongolia. The surface stations report dust in four categories: dust storm, wind-blown sand, floating dust, and no-dust. For a cloud region observed by satellite, if the surface observation is no-dust, this region is defined as CLD, and if the surface observation is dust storm, this region is defined as COD. Table 1 shows the information for the ten carefully selected dust storm cases used in this study.

[8] Histograms of the pixel-level ice cloud properties for each category from the 10 cases in Table 1 are shown in Figure 2. This figure may indicate the possible influences of dust aerosols on ice cloud properties, such as $D_e$, $\tau$ and WP. The average $D_e$ drops from 54.0 μm in the CLD regions to

48.0 μm in the COD areas. Smaller values of $D_e$ occur more frequently for both the PCOD and COD regions compared to the CLD regions. The mean $\tau$ over CLD regions (Figure 2b) is 21.9, which is 12.8 and 7.2 greater than the averaged $\tau$ of the PCOD and COD regions, respectively. Consequently, the mean WP values for PCOD and COD regions (Figure 2c) are also considerably smaller than those from CLD regions. The mean WP decreases from 396.2 g/m$^2$ to 128.7 and 230.7 g/m$^2$ for the PCOD and COD regions, respectively. The $T_e$ values (Figure 2d) for the COD regions, however, are close to the values in CLD regions, but slightly warmer ($\sim$5 K), which suggests that the cloud top heights differ by less than 1 km for these regions. The mean $T_e$ (241.3 K) in PCOD regions (Figure 2d) is higher than in the other two regions. The difference in cloud properties between the PCOD and COD regions may be due, in part, to less accurate retrievals of cloud properties along the edges of cloud decks in the PCOD regions. Under partly cloudy conditions, the satellite-retrieved cloud properties may be underestimated or over-estimated due to the presence of dust aerosol and partially cloud-filled pixels resulting in higher reflectance and warmer brightness temperatures.

[9] Figure 3 shows the mean and standard error of the cloud properties in the CLD and COD regions as a function of $T_e$. The standard error gives a rough measure of the variability of the means. Figure 3 shows that the standard errors are quite small for all three properties in all $T_e$ bins. To further evaluate the statistical significance, we also calculated the t-test for each $T_e$ bin. For all three cloud properties (De, $\tau$ and WP), the mean differences are significant at the 95% level in all $T_e$ bins except two De bins (see circled point in Figure 3a). For $\tau$ and WP, the t-test values are largest (>10) for colder clouds and decrease with increasing $T_e$. The cloud properties in COD regions represent the combined effects of upper-layer clouds and lower-layer dust aerosols. For dusty cloud tops with temperatures in the range of 230 K < $T_e \leq$ 245 K, the $D_e$ means (Figure 3a) are less than those for dust-free clouds by more than 18%. The ice crystal size of the dusty clouds is generally smaller suggesting that in COD cases, the dust aerosols are serving as ice nuclei and induce more small ice particles. The effects of dust aerosols are even more significant on $\tau$ (Figure 3b) and WP (Figure 3c). For the very cold dusty clouds ($T_e \leq$ 245 K), mean $\tau$ and WP are less than those from dust-free clouds by more than 40% and 27%, respectively, due to reduced humidity and less condensation caused by mixing of dry dust air masses with humid cloud air masses in lower atmospheric layers. Regionally averaged MOA vertical profiles of relative humidity (Table 2) show that the relative humidity is about 10% less in the COD region than in the CLD region for the middle and low atmosphere (500–

**Table 1.** Ten Dust Case Images Used in This Study

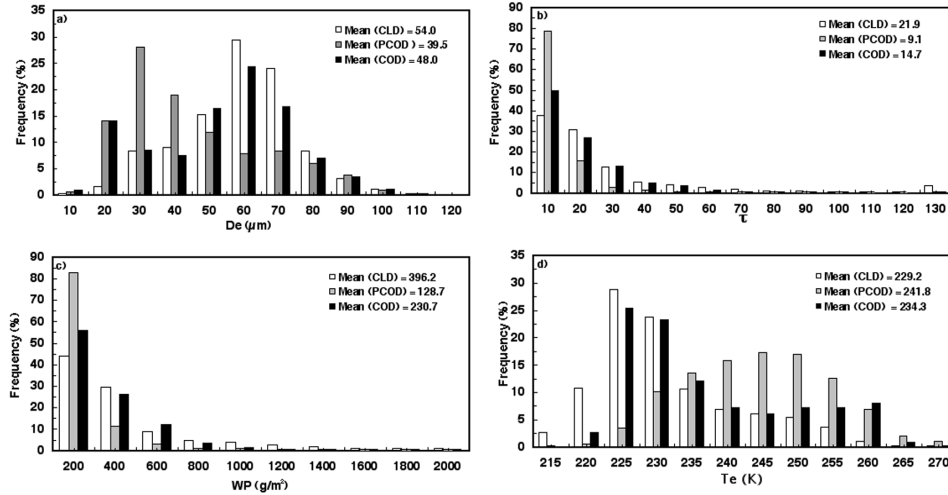| Image | Date | GMT | Lat, °N | Lon, °E | SAT |
|---|---|---|---|---|---|
| 1 | 2004/03/27 | 05:15 | 40.0–50.0 | 104.0–118.0 | Aqua |
| 2 | 2003/04/17 | 07:00 | 35.0–45.0 | 73.0–87.0 | Aqua |
| 3 | 2003/04/17 | 05:25 | 35.0–45.0 | 73.0–87.0 | Terra |
| 4 | 2003/04/09 | 06:15 | 35.0–45.0 | 72.0–86.0 | Aqua |
| 5 | 2003/04/09 | 07:50 | 35.0–45.0 | 72.0–86.0 | Terra |
| 6 | 2003/03/26 | 04:20 | 38.0–48.0 | 118.0–132.0 | Aqua |
| 7 | 2004/03/09 | 05:30 | 40.0–50.0 | 102.0–116.0 | Aqua |
| 8 | 2004/05/08 | 04:15 | 40.0–50.0 | 118.0–132.0 | Aqua |
| 9 | 2003/05/11 | 04:35 | 34.0–44.0 | 75.0–89.0 | Terra |
| 10 | 2001/04/07 | 04:20 | 33.0–43.0 | 100.0–114.0 | Terra |

**Figure 2.** Comparison of the cloud properties over the CLD region (open bar), PCOD region (gray bar), and COD region (black bar) for (a) De, (b) τ, (c) WP and (d) Te. The histogram intervals are 10 μm for Figure 2a, 10 for Figure 2b, 200 g/m² for Figure 2c, and 5 K for Figure 2d.

1000 hPa). However, in upper layers (200–500 hPa), the relative humidity in the dusty (COD and PCOD) regions is similar to that in the dust-free (CLD) regions, which suggests that the potential for generating high ice cloud hydrometeors may be the same in the upper layers.

[10] The TOA RF is defined as:

$$C_{sw} = F_{clr}^{sw} - F^{sw}$$

$$C_{lw} = F_{clr}^{lw} - F^{lw} \qquad (1)$$
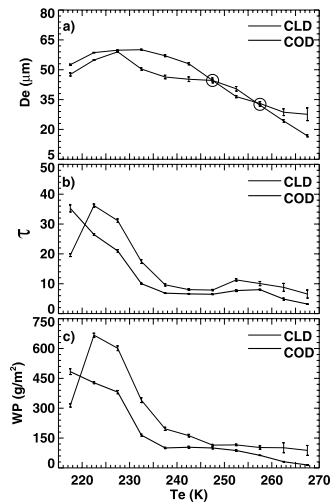
$$C_{net} = C_{sw} + C_{lw}$$



**Figure 3.** Comparison of the mean and standard error of the cloud properties over the CLD and COD regions as a function of $T_e$ for (a) $D_e$, (b) τ, and (c) WP. The vertical bars are the standard errors ($\sigma/\sqrt{N}$, where σ is the standard deviation and N is pixel number) for the CLD and COD regions, respectively. The two circled points indicate that the mean differences between CLD and COD are not significant.

where $F_{clr}^{sw}$ and $F_{clr}^{lw}$ are the CERES clear sky broadband shortwave (SW) and longwave (LW) fluxes at the TOA, respectively. $F^{sw}$ and $F^{lw}$ are the SW and LW fluxes at the TOA in the presence of dust aerosol, cloud, or both. The influences of dust on the radiation fields are calculated from the SW, LW and net fluxes of cloudy skies for the neighboring PCOD, COD, and CLD cases and binned into 100 g/m² intervals of WP. The mean statistics of the RF within each WP interval between 100 and 800 g/m² were computed and the weighted average was determined for the entire range shown in Table 3. For clouds growing in the presence of dust, the average instantaneous TOA SW RF values, −155.1 and 210.1 W/m² for the PCOD and COD regions, respectively, are about 80% and 33% weaker than that (−280 W/m²) in CLD regions. With the same IWP, the weaker SW RF in COD regions may indicate some radiation absorption by the dust aerosol since cloud particle sizes in COD regions are generally smaller than those in CLD regions. For LW RF, the dust-free cloud is around 118.9 W/m², which is 35% and 23% greater than the LW RF from PCOD and COD regions, respectively. The decrease in LW RF is a result of the greater cloud temperatures of the dusty clouds. The mean instantaneous TOA net RF for the CLD region is about −161.6 W/m², which is about 30–50% greater than the value from the dusty cloud (PCOD and COD) regions and about 4 times as large as that of DUST regions. If the diurnal cycle of the forcing is considered, the estimated mean net RF is −21, 0, −14 and 3 W/m² for CLD, PCOD, COD and DUST regions, respectively. Thus, the existence of dust under clouds significantly reduces the cooling effect of clouds. The reduced cooling effects of dust for the PCOD (21 W/m²) and COD (7 W/m²) regions can be considered as actual warming effects due to dust aerosols. Since the long-term averaged dust storm

**Table 2.** Comparison of the Averaged Relative Humidity (%) Between Different Regions

|  | Dust | CLD | PCOD | COD |
|---|---|---|---|---|
| 200–500 hPa | 43.5 | 58.5 | 59.9 | 66.9 |
| 500–1000 hPa | 36.3 | 57.5 | 46.1 | 47.6 |

**Table 3.** Comparison of the Averaged RF (W/m$^2$) at the TOA

|  | Dust | CLD | PCOD | COD |
|---|---|---|---|---|
| SW RF | −89.9 | −280.1 | −155.1 | −210.1 |
| LW RF | 47.9 | 118.9 | 77.2 | 91.5 |
| Net RF | −42.1 | −161.6 | −77.9 | −118.6 |

frequency of occurrence based on surface meteorological station observations is about 3.7%, assuming the frequencies of occurrence of PCOD, COD and DUST in dusty cases are the same, the averaged climate forcing (warming) of dust storms is about 0.4 W/m$^2$.

## 4. Conclusions and Discussions

[11] This study shows the effect of Asian dust aerosols on ice cloud properties and TOA RF. Satellite data may not be the perfect means to detect the effect of dust on clouds but is the only one conveniently available. Analysis of the satellite observations shows that the D$_e$ values of dusty clouds are considerably smaller than those from dust-free clouds. It suggests that dust aerosols may act as cloud condensation nuclei and cause changes in the size of ice cloud particles. *DeMott et al.* [2003] provided evidence for the strong ice nucleating function of Saharan dust aerosols as measured at long distances from the source. The current results also show that the τ and WP of dusty clouds are much less than those from dust-free clouds. Previous studies [*Twomey et al.*, 1984; *Albrecht*, 1989] indicated constant or increased cloud liquid WP associated with high aerosol concentrations for water clouds over oceans. Current results suggest a different effect of dust aerosols on relatively dry upper-level air masses, high clouds, and ice cloud condensation over arid or semi-arid regions. The key issue may be related to the semi-direct effect or cloud evaporation. As dust aerosols cool the Earth's surface and heat the aerosol layer, the atmospheric stability within and above the boundary layer is reduced, resulting in enhanced vertical motion and increased airborne dust. Additionally, dust aerosols can cause evaporation of cloud droplets (semi-direct effect). This leads to reduced cloud water path and affects the RF. However, in terms of meteorological states, the clouds in dusty regions are drier (Table 2) and (cloud top) warmer (Figure 2d) than those in non-dusty regions, the comparison between De in dusty and non-dusty regions is not under the exactly same conditions. From in-situ observations, effective ice crystal sizes are generally larger in warmer conditions than those in colder environments [*Heymsfield and Platt*, 1984]. Thus, we attribute the size change (i.e., reducing cloud particle size in dusty regions) to the drier conditions. The dehydration process of wet dust precipitation may be one of the possible candidates causing dry conditions. Another obvious factor, causing dry conditions, can be the air mass source of the dust clouds. The dust layers in the source regions are likely to have dry air masses. In this case, the impact of dust aerosols on RF becomes very complex. Since the PCOD, COD and CLD regions in each case are determined from the same synoptic weather system, the meteorological conditions for these regions are assumed to be similar. The differences in radiative properties such as

radiative fluxes, optical depth and particle size are considered as dust effects. For DUST regions, the dust aerosol has a cooling effect at the TOA in daytime and net warming when both day and night are considered. These aerosols also cancel or reduce the cloud cooling effect at the TOA in PCOD and COD regions due to decreasing water path. If confirmed, the net RF (0.4 W/m$^2$) of dust storms estimated from the current study will be the strongest aerosol forcing in the studied region during dust storm seasons, and have profound warming influences on the atmospheric general circulation and climate.

## References

Ackerman, S. A. (1997), Remote sensing aerosols using satellite infrared observations, *J. Geophys. Res.*, *102*(D14), 17,069–17,080.

Ackerman, A. S., et al. (2000), Reduction of tropical cloudiness by soot, *Science*, *288*, 1042–1047.

Albrecht, B. A. (1989), Aerosols, cloud microphysics, and fractional cloudiness, *Science*, *245*, 1227–1230.

Bréon, F.-M., et al. (2002), Aerosol effect on cloud droplet size monitored from satellite, *Science*, *295*, 834–838.

DeMott, P. J., K. Sassen, M. R. Poellot, D. Baumgardner, D. C. Rogers, S. D. Brooks, A. J. Prenni, and S. M. Kreidenweis (2003), African dust aerosols as atmospheric ice nuclei, *Geophys. Res. Lett.*, *30*(14), 1732, doi:10.1029/2003GL017410.

Gu, Y., W. I. Rose, and G. J. S. Bluth (2003), Retrieval of mass and sizes of particles in sandstorms using two MODIS IR bands: A case study of April 7, 2001 sandstorm in China, *Geophys. Res. Lett.*, *30*(15), 1805, doi:10.1029/2003GL017405.

Heymsfield, A. J., and C. M. R. Platt (1984), A parameterization of the particle size spectrum of ice clouds in terms of the ambient temperature and ice water content, *J. Atmos. Sci.*, *41*, 846–855.

Levi, Y., and D. Rosenfeld (1996), Ice nuclei, rainwater chemical composition, and static cloud seeding effects in Israel, *J. Appl. Meteorol.*, *35*, 1494–1501.

Minnis, P., et al. (1995), Cloud optical property retrieval (Subsystem 4.3), in *Clouds and the Earth's Radiant Energy System (CERES) Algorithm Theoretical Basis Document, Volume III: Cloud Analyses and Determination of Improved Top of Atmosphere Fluxes (Subsystem 4)*, NASA Tech. Rep., NASA RP 1376, 135–176.

Minnis, P., et al. (1998), Parameterization of reflectance and effective emittance for satellite remote sensing of cloud properties, *J. Atmos. Sci.*, *55*, 3313–3339.

Rosenfeld, D., and R. Nirel (1996), Seeding effectiveness—The interaction of desert dust and the southern margins of rain cloud systems in Israel, *J. Appl. Meteorol.*, *35*, 1502–1510.

Rosenfeld, D., et al. (2001), Desert dust suppressing precipitation: A possible desertification feedback loop, *Proc. Natl. Acad. Sci. U. S. A.*, *98*(11), 5975–5980.

Sokolik, I. N. (2002), The spectral radiative signature of wind-blown mineral dust: Implications for remote sensing in the thermal IR region, *Geophys. Res. Lett.*, *29*(24), 2154, doi:10.1029/2002GL015910.

Sokolik, I. N., O. B. Toon, and R. W. Bergstrom (1998), Modeling the radiative characteristics of airborne mineral aerosols at infrared wavelengths, *J. Geophys. Res.*, *103*(D8), 8813–8826.

Twomey, S., et al. (1984), An assessment of the impact of pollution on global cloud albedo, *Tellus, Ser. B, 36*, 356–366.

―――――――――

K. Ayers and Y. Yi, Analytical Services & Materials, Inc., One Enterprise Parkway, Hampton, VA 23666, USA.

Y. Hu, B. Lin, and P. Minnis, NASA Langley Research Center, MS 420, Hampton, VA 23681–2199, USA.

J. Huang and T. Wang, College of Atmospheric Sciences, Lanzhou University, Lanzhou, 730000, China. (j.huang@larc.nasa.gov)

S. Sun-Mack, Science Applications International Corporation, One Enterprise Parkway, Hampton, VA 23666, USA.